

Dynamic Polymer Free Volume Monitored by Single-Molecule Spectroscopy of a Dual Fluorescent Flapping Dopant

Yuma Goto, Shun Omagari, Ryuma Sato, Takuya Yamakado, Ryo Achiwa, Nilanjan Dey, Kensuke Suga, Martin Vacha,* and Shohei Saito*



Cite This: <https://doi.org/10.1021/jacs.1c06428>



Read Online

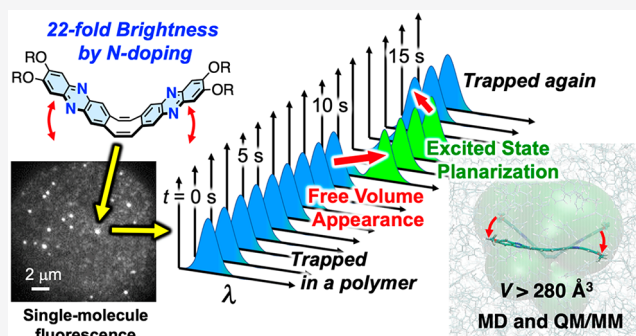
ACCESS |

Metrics & More

Article Recommendations

Supporting Information

ABSTRACT: Single-molecule spectroscopy (SMS) of a dual fluorescent flapping molecular probe (N-FLAP) enabled real-time nanoscale monitoring of local free volume dynamics in polystyrenes. The SMS study was realized by structural improvement of a previously reported flapping molecule by nitrogen substitution, leading to increased brightness (22 times) of the probe. In a polystyrene thin film at the temperature of 5 K above the glass transition, the spectra of a single N-FLAP molecule undergo frequent jumps between short- and long-wavelength forms, the latter one indicating planarization of the molecule in the excited state. The observed spectral jumps were statistically analyzed to reveal the dynamics of the molecular environment. The analysis together with MD and QM/MM calculations show that the excited-state planarization of the flapping probe occurs only when sufficiently large polymer free volume of more than, at least, 280 Å³ is available close to the molecule, and that such free volume lasts for an average of 1.2 s.



INTRODUCTION

Polymer free volume is a practical concept for interpreting polymer properties connected to the fraction of unoccupied volume.¹ While arbitrary definition of “free volume” often led to controversy, a quantitative evaluation of polymer free volume is important for developing membrane materials as well as packing materials for chromatography that adsorb, diffuse, and separate small molecules.² Local free volume moves from moment to moment due to thermal fluctuation of surrounding polymer chains. To evaluate the free volume directly and quantitatively, several approaches have been established such as positron annihilation lifetime spectroscopy (PALS),³ inverse gas chromatography (IGC),⁴ ¹²⁹Xe NMR spectroscopy,⁵ and molecular probe.^{6–8} In recent years, some studies have been reported which compare experimental results with molecular dynamics (MD) simulation.⁹ However, real-time monitoring of the local free-volume dynamics has only been achieved by single-molecule spectroscopy (SMS) analysis of conformationally flexible probes.¹⁰ In this literature, single-molecule fluorescence lifetime has been analyzed because the conformational change of the fluorescent probe, twisted peryleneimide, results in very little spectral difference. This work is an example of the great potential that the SMS technique holds for spatially resolved dynamic studies of polymers and soft matter in general.¹¹ Apart from free-volume probing, SMS has been used, e.g., to analyze heterogeneity of local relaxation processes of polymers near glass transition

temperature (T_g),^{12–14} to characterize diffusion in solutions or melts,^{15,16} or to monitor polymerization reactions on molecular level.^{17,18} In particular, the SMS method could be an attractive alternative to tracking the dynamics of the polymer free volume because of its high location specificity, suitable dynamic range, noninvasive nature, and relatively affordable and simple optical instrumentation. Here, we succeeded in demonstrating such free-volume monitoring by developing a new flexible fluorophore, nitrogen-embedded flapping molecule (N-FLAP), which shows dual fluorescence (FL) spectrum depending on the bent/planar conformations (Figure 1). In comparison with the previously reported flapping anthracene,¹⁹ the nitrogen-embedded molecular framework led to much improved FL brightness as well as high photostability, when excited by a visible light. With this unique molecular probe physically doped in polystyrenes, SMS study has been performed to demonstrate that dynamic nanoscale changes of polymer free volume can be monitored in real time by following local environment-dependent spectral changes of a single N-FLAP molecule. This is the first

Received: June 21, 2021

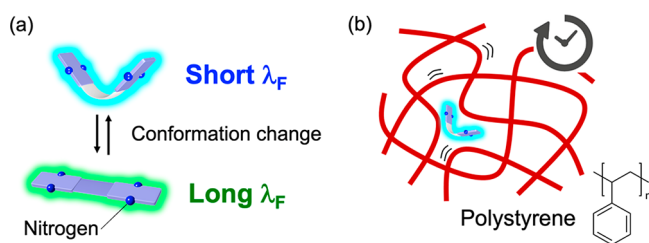


Figure 1. (a) Nitrogen-embedded flapping fluorophore (N-FLAP) as a bright dual-fluorescent probe and (b) real-time analysis of polystyrene free volume using the N-FLAP dopant. λ_F : Fluorescence wavelength.

application of a dual emissive molecule²⁰ to the free-volume monitoring in a single-molecule level.

EXPERIMENTAL SECTION

Synthesis and Characterization of N-FLAP Probe. A previously reported flapping anthracene (FLAP in Figure 3a) works as a fluorescent viscosity probe that shows polarity-independent dual FL.¹⁹ The flapping anthracene undergoes a bent-to-planar conformational change in the lowest singlet excited state (S_1), while it instantly returns to the most stable bent form in the singlet ground state (S_0). Since the S_1 planarization is partially suppressed in a viscous media, ratiometric FL analysis is available for quantifying local viscosity. The flapping anthracene has only weak absorption bands in the visible range, and low photostability has been demonstrated when excited by a strong UV light.²¹ This photodegradation behavior is a serious shortcoming for the application to the single-molecule FL analysis, in which continuous FL emission is required for counting photon signals.²² Particularly for the spectroscopic study, bright FL as well as the high photostability is expected for accumulating photons with respective energies. Here, we designed a flapping phenazine (N-FLAP) probe, in which reactive 9 and 10 positions of the original anthracene moieties were capped by nitrogen atoms to suppress undesired photoreactions.

N-FLAP was newly prepared by the Pd-catalyzed phenazine synthesis.²³ The coupling reaction of compounds **1**²⁴ and **2** followed by an in situ oxidation provided N-FLAP in 45% yield (Figure 2a).

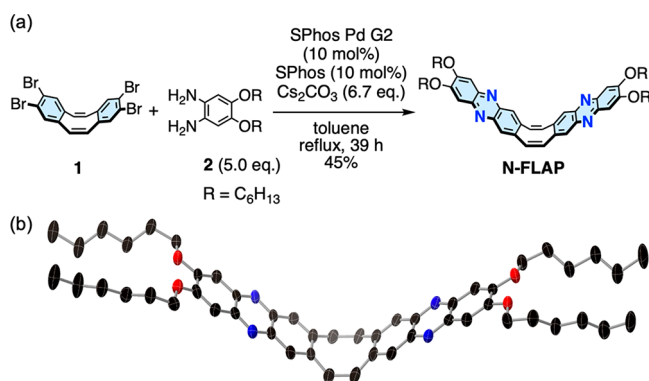


Figure 2. (a) Synthesis of N-FLAP. SPhos Pd G2: A commercially available second generation SPhos precatalyst. (b) Single crystal X-ray structure analysis. Thermal ellipsoids were drawn at the 50% probability level. Hydrogen atoms were omitted for clarity.

Single-crystal X-ray diffraction analysis revealed a V-shaped structure of N-FLAP with the cyclooctatetraene (COT) bending angles, defined in Figure 3d, of $\theta = 36.5^\circ$ and 39.2° (Figure 2b).

Optical Properties of N-FLAP Probe. Absorption bands of N-FLAP were red-shifted (415 nm in CH_2Cl_2) in comparison with those of the previously reported flapping anthracene (Figure 3a). Remarkably, the molar absorption coefficient (ϵ) in the visible region

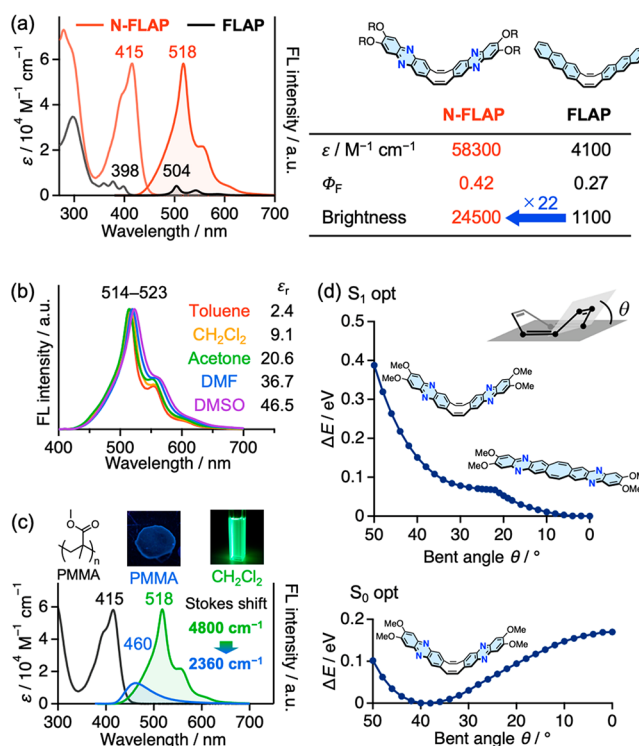


Figure 3. (a) Absorption and FL spectra of N-FLAP, compared with those of the previously reported flapping anthracene (FLAP) in CH_2Cl_2 . Relative area of the FL spectra is proportional to the brightness of the probes. (b) Solvent dependence (ϵ_r : relative permittivity) and (c) environment dependence in the FL spectra of N-FLAP. Excitation wavelength $\lambda_{\text{ex}} = 365$ nm. (d) Calculated energy profiles of N-FLAP' in the excited state (S_1) and the ground state (S_0). With the fixed COT bending angle θ (see inset), structural optimizations were performed by (TD)-DFT calculations at the TPSSH/6-31+G(d) level.

increased more than 10-fold ($5.8 \times 10^4 \text{ M}^{-1} \text{cm}^{-1}$) compared with that of the flapping anthracene ($4.1 \times 10^3 \text{ M}^{-1} \text{cm}^{-1}$ at 398 nm). The difference in the molar absorption coefficients was supported by time-dependent density functional theory (TD-DFT) calculations. A model structure, N-FLAP', was treated for the calculations, in which the terminal OC_6H_{13} substituents of N-FLAP were replaced by OCH_3 groups. Strong visible absorption of an allowed transition ($f \approx 0.5$) is expected for N-FLAP', while only a weak visible absorption with small oscillator strength ($f \approx 0.06$) is assigned for FLAP (Figure S17). In addition, molecular orbital (MO) energy levels originating from the phenazine wings of N-FLAP' become lower than those of the anthracene wings of FLAP by the nitrogen substitution. The lower LUMO level may lead to the suppression of photo-oxidation in N-FLAP.

N-FLAP showed a green fluorescence peaked at 518 nm with a large Stokes shift of 4800 cm^{-1} in CH_2Cl_2 , indicating a conformational planarization in the lowest singlet excited state (S_1), as seen in other flapping anthracenes (Figure 3a). Absolute fluorescence quantum yield of N-FLAP ($\Phi_F = 0.42$) was higher than that of FLAP ($\Phi_F = 0.27$).²⁵ Thus, the brightness of N-FLAP, defined as $\epsilon \times \Phi_F$, is 22 times higher than that of FLAP (Figure 3a, inset table), overcoming the drawbacks of the previous FLAP probe for the SMS use. Polarity independence in the FL spectra of N-FLAP was confirmed in various solvents (toluene, CH_2Cl_2 , acetone, DMF, and DMSO) covering a wide range of relative permittivity (ϵ_r) from 2.4 (toluene) to 46.7 (DMSO) at room temperature. The peak wavelength of the FL band shifted within a small range of 514–523 nm (Figure 3b), suggesting a negligible charge-transfer character in the excited state. When dispersed in a rigid poly(methyl methacrylate) (PMMA) matrix, N-FLAP emitted a blue FL ($\lambda_F = 460$ nm, $\Phi_F =$

0.13) with smaller Stokes shift of 2360 cm^{-1} (Figure 3c). This drastic FL chromism was also observed with increasing viscosity of a 2-methyltetrahydrofuran solution at lower temperatures (Figure S7d). These behaviors indicate that the conformational planarization of N-FLAP in S_1 is suppressed in the rigid (highly viscous) environments.

To support the explanation of conformational dynamics in S_1 , (TD-)DFT calculations were conducted. Although the calculation results are very sensitive to the selected levels of theory (SI, Section 4.1), here, we chose the TPSSh/6-31+G(d) level for better interpreting the experimental results. Potential energy profiles of N-FLAP' were delineated with changing the COT bending angle θ by 2 degrees in the ground state (S_0) and the excited state (S_1) (Figure 3d). In S_0 , the optimized structure of N-FLAP' takes a V-shaped form ($\theta = 38.8^\circ$), while the planar structure gives a transition state. In contrast, the most stable geometry in S_1 is the planar conformation ($\theta = 0^\circ$) at which the S_0 - S_1 transition is allowed ($f \approx 0.3$). The calculation results rationalize the observed green bright FL with a large Stokes shift (Figure S15e). In addition, an electronic configuration switch was predicted during the conformational planarization in S_1 , as was the case with reported FLAP.^{19,25}

Thermal and Viscoelastic Properties of Host Polymers. High molecular-weight polystyrene (high MW PS; $M_w \approx 192000$) and low MW PS ($M_w \approx 850$) were selected for this study. Glass transition temperatures (T_g) of high MW PS and low MW PS were determined to be 102 and 18 °C, respectively, based on inflection points of the DSC profiles in the cooling process. Dynamic viscoelasticity measurements showed that the polystyrenes hardened at around T_g , and the storage modulus (G') was $0.9 \times 10^9\text{ Pa}$ (65 °C and below) for high MW PS and $7 \times 10^7\text{ Pa}$ (25 °C) for low MW PS (Figure 4).

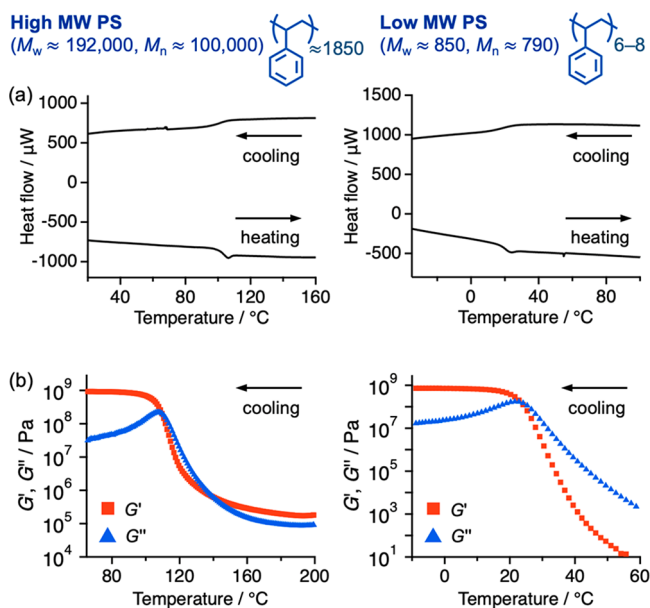


Figure 4. (a) DSC profiles and (b) temperature-dependent dynamic viscoelasticity of the host polymers, high MW PS (left) and low MW PS (right). Scan rate: 5 °C/min for both measurements. G' : storage modulus. G'' : loss modulus.

The molecular weight between entanglement points (M_e) has been reported as 18700 for polystyrene melt.²⁶ Therefore, the high MW PS is expected to have *ca.* 10 entanglement points per a single polymer chain, while the low MW PS has no entanglement point. The M_e value of polystyrene corresponds to 180 monomer units and thus 360 covalent bonds in the polymer main chain. According to the freely rotating chain (FRC)²⁷ model, the expected distance between entangled points can be roughly estimated as 4.1 nm ($=0.154\text{ nm} \times \sqrt{2} \times 360$). Here, 0.154 nm is a saturated C-C covalent bond length. In addition, the expected end-to-end distances

for the high and low MW PS can be calculated as 13 and 0.9 nm, while the length of the bent N-FLAP' conformation is about 2 nm.

Due to the small molecular weight of the low MW PS (which can be even regarded as a mixture of oligostyrenes), the end groups would play a significant role. Then, we analyzed the commercially available low MW PS sample by NMR spectroscopies and high-resolution APCI (atmospheric pressure chemical ionization) mass spectrometry (see the details in the final chapter of the SI). In conclusion, we have reasonably determined the terminal structures as a *sec*-butyl group and a hydrogen atom, which are probably attached in the process of anion polymerization.²⁸ On the basis of the analyses, tacticity of the oligostyrene was found to be atactic, and the oligomer sample is mainly composed of the 6–8 mers. As a result, no specific interaction between the terminal end groups and N-FLAP is expected in the following study.

Methods of Single-Molecule Fluorescence Spectroscopy.

For single-molecule FL studies, toluene solutions of the host PS polymers and a trace of N-FLAP were prepared (the concentration of N-FLAP: 10^{-9} M) and then spin-coated to form *ca.* 100 nm thick sample films on glass substrates. After annealing the PS films by heating above T_g for approximately 30 min, we carried out the SMS experiments at 23 °C in a N_2 atmosphere on top of an inverted FL microscope equipped with an imaging spectrograph (Figure 5a).

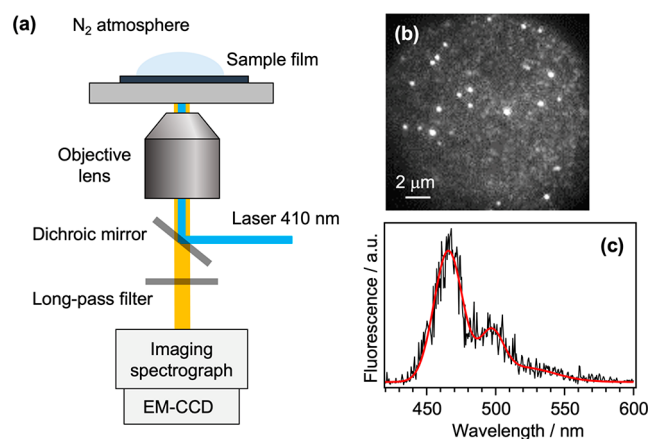


Figure 5. (a) Scheme of the experimental setup. (b) An example of microscopic FL image, in which the bright spots correspond to the N-FLAP single molecules dispersed in a spin-coated polystyrene thin film. (c) An example of single-molecule FL spectrum of the N-FLAP probe.

Switching to the spectral mode of the spectrograph enables wavelength dispersion of FL signal from individual molecules, the dynamics of which can be then monitored for extended periods of time. Figure 5b,c show a typical FL image of the dispersed N-FLAP molecules and an example of a single-molecule FL spectrum, respectively.

RESULTS AND DISCUSSION

Results of Single-Molecule Fluorescence Spectroscopy. SMS of N-FLAP in the high MW PS was performed first. As mentioned above, the high MW PS has its T_g at 102 °C (Figure 4) and represents rigid environment for the N-FLAP molecule. An example of time evolution of single-molecule FL spectrum in the high MW PS is shown in Figure S25. At the measurement temperature of 23 °C (much lower than T_g), the molecule showed a spectrally stable emission with a FL peak (0–0 vibrational band) at 445 nm. The single-molecule spectrum has a clearly resolved vibronic structure, while ensembles of N-FLAP molecules in bulk PS films provided only averaged broad structureless spectrum mainly in a blue

region (420–520 nm) (Figure S25), This behavior is typical for most of the N-FLAP molecules trapped in the high MW PS, indicating almost complete suppression of the conformational planarization of N-FLAP in S_1 .

Next, SMS in the low MW PS was conducted. Since the measurement temperature of 23 °C is slightly above its T_g (18 °C), the PS chains start undergoing segmental relaxation in the form of micro-Brownian motion. The dynamic nature of the polymer matrix is reflected in the spectroscopic behavior of the individual N-FLAP molecular probes. A typical example of the time evolution plot is shown in Figure 6a. This molecule stayed

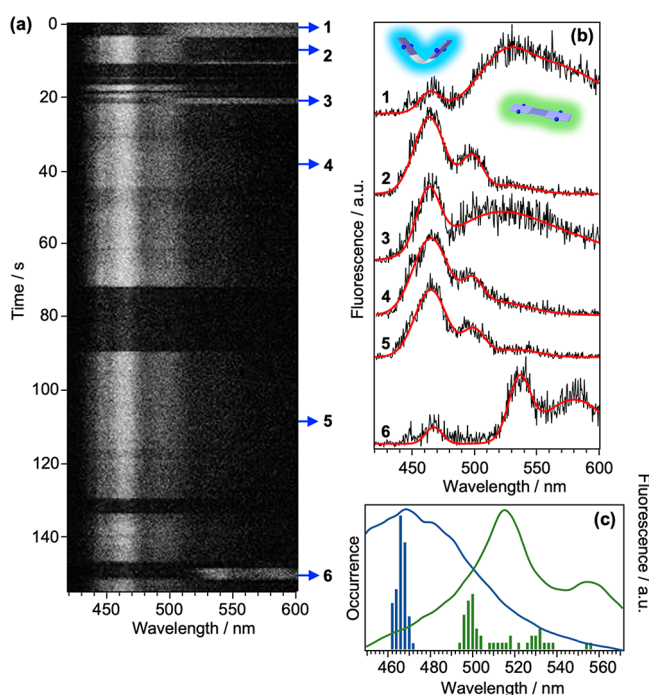


Figure 6. (a) Time evolution for the FL spectra of a single N-FLAP molecule dispersed in the low MW PS matrix. The vertical axis indicates measurement time (from top to bottom). Each horizontal line represents a FL spectrum with the signal intensity shown in gray scale. Numbers (1–6) are assigned for each time range and (b) the corresponding FL spectra, fitted with a sum of three Gaussian functions. (c) Histogram of the single-molecule FL peak wavelengths analyzed from 105 individual spectra. FL peaks at shorter wavelengths are shown as blue bars, while longer ones counted as green bars. Ensemble FL spectra of N-FLAP in a drop-cast high MW PS film (blue solid line) and in a PS-containing toluene solution (green solid line) were also shown.

in the blue form most of the time with the peak position at 464 nm, but occasionally undergoes a spectral jump to the green form, reminiscent of the solution-phase FL spectra with a peak top around 520 nm (Figure 3b). In other N-FLAP molecules (Figure S26), the spectral jumps occurred with varying frequency. There is a wide distribution of times for which the molecule stays in the green form. The observed FL peak wavelengths also showed a large variance in the green range (490–540 nm). Such variety of the green FL spectra is evident even for the same N-FLAP molecule in different time ranges (see the spectra 1, 3, and 6 in Figure 6b). The spectral distribution is characterized by plotting a histogram of the FL peak positions based on the analysis of 105 spectra (Figure 6c). When overlaid with ensemble FL spectra of N-FLAP molecules dispersed in a rigid high MW PS matrix and in a toluene

solution of PS, there is a good correspondence between the single-molecule and ensemble spectral regions both for the blue and green FL bands. Regarding the ensemble spectra in low MW PS matrixes; see Figure S11.

Discussion for Dynamic Single-Molecule Fluorescence. The appearance of the green FL band of the flapping probe in solution is a consequence of the low viscosity environment which enables the planarization of the chromophore in S_1 .¹⁹ In the solid state, the flapping molecule requires certain free space for the planarization to happen.²⁹ In polymers, this free space should be closely related to the concept of free volume,¹ although there is a non-negligible difference between the “free volume” values estimated by molecular probes and by PALS.¹⁰ (PALS studies generally report smaller volumes than those reported by molecular probe studies.) In a polymer film above the glass transition temperature T_g , segmental relaxation causes dynamical changes to the free volume which can repeatedly form and disappear around the N-FLAP probe. This temporary appearance of the free volume would enable the excited-state planarization of N-FLAP and emission of the green band, and its disappearance would cause a return to the blue emission (Figure 7a).

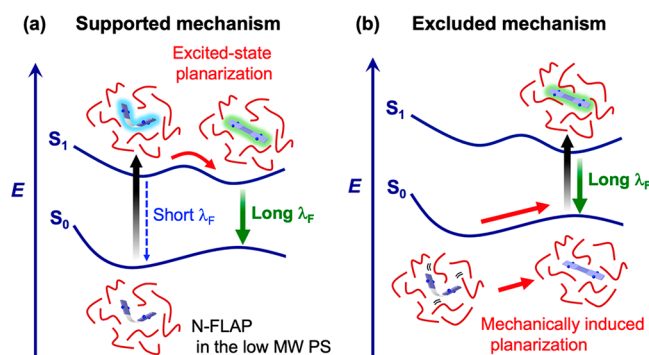


Figure 7. Two possible mechanisms for the single-molecule spectral dynamics in Figure 6. (a) One possibility is that the excited-state planarization of N-FLAP is allowed only when the free volume temporarily appeared around the N-FLAP probe. (b) The other is that compulsory planarization is mechanically induced by dynamic segmental motions of the surrounding polymer chains.

Alternatively, the segmental micro-Brownian motion of the surrounding polymer chains itself could also cause mechanical planarization of N-FLAP in the ground state, which would also result in the green emission from the planarized N-FLAP in a confined space (Figure 7b). To distinguish between these two possible mechanisms, i.e., existence of a free volume vs segmental motion-induced planarization, we carried out control experiments in both high and low MW PS using another flapping dye, which has been reported as a flexible mechanophore that does not undergo spontaneous excited-state planarization even in solution.³⁰ The flexible mechanophore (A-FLAP) has bulky triisopropylsilyl (TIPS) ethynyl groups introduced on the anthracene moieties (Figure S27), and when mechanically compressed in a crystalline phase it attains the planar conformation and emits red-shifted fluorescence. Calculated energy barrier for the mechanical planarization of A-FLAP in S_0 is practically same as that of N-FLAP. The SMS results of A-FLAP in both high and low MW PS showed that, irrespective of the matrix, the single-molecule spectra are of the short-wavelength form, namely, the bent conformation of A-FLAP is preserved (Figure S27). This result

means that even in the rubbery-state PS film above T_g the segmental motion does not cause mechanical planarization of the A-FLAP or N-FLAP dyes, and that the observed green FL of N-FLAP is emitted via the excited-state planarization during the temporal appearance of the local free volume in the low MW PS film (Figure 7a).

To get an insight into the dynamics of free volume formation and disappearance, we further analyzed the spectral time traces of single N-FLAP molecules in the low MW PS. Specifically, we evaluated the time intervals for which the molecule stayed in the blue form before jumping to the green form and, separately, the intervals for which the molecule stayed in the green form before reversing back to the blue one. Histograms of both intervals (Figure 8) show exponential distributions which, when fitted with single-exponential functions, provide the characteristic duration times of the blue form (τ_b) of 10.4 ± 0.5 s and of the green form (τ_g) of 1.2 ± 0.1 s. In the picture of polymer free volume, these results

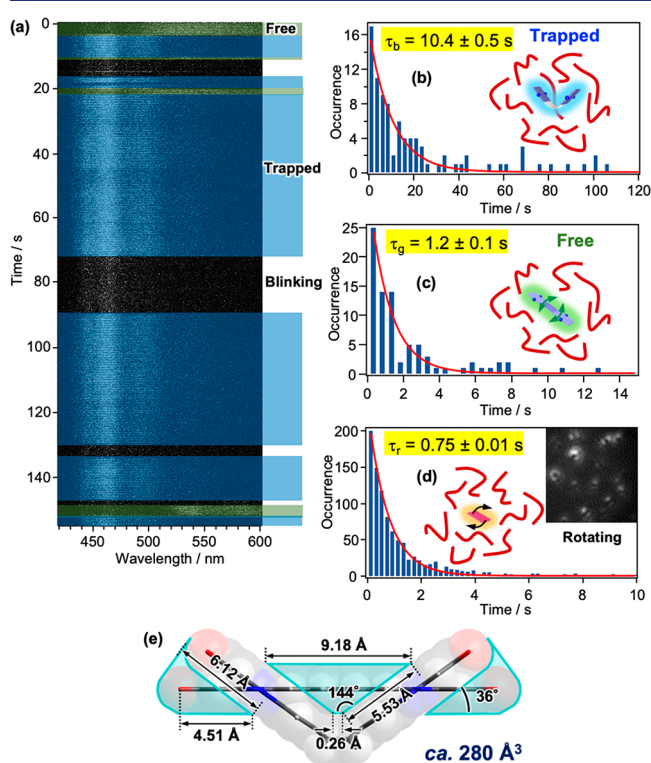


Figure 8. (a) Time evolution of single-molecule FL spectra of N-FLAP in the low MW PS; the shaded areas indicate the short (blue) and long (green) wavelength forms. (b) Histogram of time duration of the blue spectral form before switching to the green one, constructed from 90 data points of different 21 molecules and fitted with an exponential. (c) Histogram of time duration of the green spectral form before switching to the blue one, constructed from 84 data points of different 21 molecules and fitted with an exponential. (d) Histogram of reorientation times of single PDI molecules in the low MW PS constructed from 955 events and fitted with an exponential. Inset shows an example of defocused FL image. Overall, 73 out of 130 PDI molecules measured in the low MW PS showed the rotational motion. PDI: *N,N'*-di-*n*-octyl-3,4,9,10-perylene-tetracarboxylic diimide. (e) Estimated minimum volume required for the excited-state planarization of N-FLAP'. In the space-filling models, terminal alkyl chains were not considered because conformationally flexible moieties generally do not disturb dynamic motions of rigid chromophores.³³

show that it takes an average of 10.4 s for a sufficiently large free volume to form around the N-FLAP molecule, and that this volume lasts for an average of 1.2 s before it disappears. It is only during the presence of the sufficient free volume that the N-FLAP molecule can undergo repeated planarization after each excitation and emit the green fluorescence continuously for several seconds. We have estimated that the minimum free volume required for the N-FLAP planarization is *ca.* 280 \AA^3 (green part in Figure 8e; see also Figure S32). Here, the volume swept out during planarization has been estimated. The green part is composed of the terminal part swept out by the flapping wings and the central part swept out by the planarized COT. From the superimposed model of the bent and planar structures with the center of gravity fixed, the terminal and central parts were roughly estimated as 170 and 110 \AA^3 , respectively. The sum of these two parts gave 280 \AA^3 . This estimate is comparable with upper limits of distributions of free volume in PS measured by positron annihilation³¹ or fluorescence photochromic probes,⁶ although the existence of the N-FLAP probe itself could have an influence for the estimation of polymer free volume and therefore the result should be carefully compared with other measurement methods. The large difference between the two characteristic times τ_b and τ_g reflects the formation and disappearance mechanisms of the large free volume. The formation is associated with cooperative motion of several segments of chains surrounding the molecule. However, once the free volume is formed, a motion of a single segment is sufficient for its destruction. The τ_g should therefore reflect the segmental relaxation time (α -relaxation) whereas the τ_b is longer due to the cooperative nature of the formation process. The τ_g of 1.2 s is well within the range of α -relaxation times measured by dielectric spectroscopy for PS with a varying range of molecular weight around the T_g temperature.³²

It is worth noting that the time scale of the photophysical excitation events is much shorter than the segmental motion of the polymer chain. Considering the photon density of the laser, the average period between these excitation events per molecule has been estimated to be *ca.* 0.2 ms. Further, it takes 300–500 ms to accumulate enough fluorescence signal to obtain fluorescence spectra (such as the individual frames in Figure 6). Free volume change occurs on the time scale of the segmental motion (several seconds). On the basis of the above, we propose that the segmental motion determines the local free volume around the probe, and the fast structural dynamics of the excited N-FLAP is dependent on the degree of the local free volume. During the periods of sufficiently large free volume, N-FLAP repeats the fast photophysical cycle of (1) S_0 to S_1 excitation at the bent form, (2) spontaneous planarization in S_1 , (3) fluorescence emission (or nonradiative decay) giving the planar form in S_0 , and (4) spontaneous bending in S_0 . Thus, the long-wavelength spectrum is observed. By contrast, during the period of small free volume, excited N-FLAP cannot planarize in S_1 and therefore the accumulated fluorescence signal of the bent conformation gives the short-wavelength spectrum.

There is also a way of directly measuring the local relaxation times by monitoring reorientation of single-molecule fluorescent probes doped in the film.^{13,14,34} As a reference, we have carried out such measurement using a perylene diimide (PDI) dye and the technique of defocused imaging^{35,36} (Figure 8d). However, rather than analyzing the reorientation process by plotting the autocorrelation function and fitting it with the

stretched exponential (KWW) function,^{10,13} we chose to plot a distribution of reorientation times for a statistical sample of single molecules. For this purpose, reorientation time is defined as the time for which the molecule stays in a certain orientation before reorientation, by more than 30°, occurs. Since such reorientation supposedly reflects a segmental motion of a nearby PS chain, this analysis enables direct comparison with the distribution of the τ_g times obtained for the N-FLAP molecules. The results (presented also in Figure S28) show that the distribution of reorientation times is also exponential, and fitting with a single exponential function provides a characteristic reorientation time τ_r of 0.75 s. This value is generally in very good agreement with the 1.2 s of $\tau_{g'}$ and indicates that the lifetime of the free volume is indeed determined by the segmental motion.

While both τ_b and τ_g show overall exponential distributions, there is an interesting trend observed from traces of different individual molecules in Figure S26. At least within the observation time of 160 s, there appears to be a kind of local memory effect in spectral traces, i.e., a molecule which tends to have short τ_g and long τ_b shows this behavior throughout the observation time, and the same is true for long τ_g and moderate τ_b (Figure S26b,d, respectively). This observation points to spatial heterogeneity of the α -relaxation process that has been observed before in poly(*n*-butyl methacrylate) (PnBMA) near T_g ¹⁰ as well as in supercooled liquids³⁷ and that persists for minutes of the measurement times. The effect of glass/polymer interface and polymer film surface with air are the most probable origins of the observed memory effect. For example, a thin immobile layer at the interface and thin liquid-like layer at the polymer film surface has been reported,¹⁴ which would be consistent with the observations of very short or very long green emitting forms, respectively. Similarly, surface mobile layer was used to explain the observed diffusion.³⁸

We note that, in principle, the observed spectral dynamics of the N-FLAP dye could be alternatively explained by assuming that the dye-surrounding polymer becomes temporarily liquid-like, enabling the excited-state planarization in the same way as in a solution. However, such local liquid-like state is not very probable at or near T_g . In addition, it should also be observable in the PDI reorientation experiment where it would lead to periods of fast rotation, none of which has been observed. This mechanism of green-emission formation would be more relevant at higher temperatures close to the melting point.

MD Simulations and QM/MM Calculations. To validate the proposed mechanism, we also performed calculations considering the host polymer (500 entangled chains of the low MW PS). First, classical MD simulations of the low MW PS with a single N-FLAP' molecule were conducted to obtain a PS geometry that contains the sufficient void space for the flapping motion of N-FLAP'. While such the geometry was not obtained in the time range of 1000 ns when simulated at 25 °C, those geometries were generated by the simulation at high temperature (see SI for details). Then, the N-FLAP' molecule with the fixed COT bending angle was placed in the void space, and additional MD calculations were conducted only for the PS chains that were spatially overlapped with N-FLAP'. After that, constraint geometry optimization was performed with the QM/MM^{39,40} (quantum mechanics/molecular mechanics) calculations (Figure 9a). The PS geometry was fixed and treated with the MM model, while the electronic structure of N-FLAP' was considered with the QM model. After several trials at different calculation levels, it was found

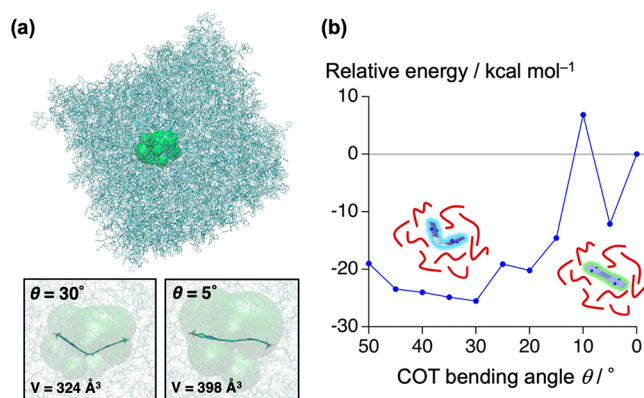


Figure 9. (a) Structural model for the QM/MM calculations, in which N-FLAP' is placed at the center of the low MW PS (500 polymer chains). Green void (calculated by POVME 2.0⁴¹) corresponds to the free volume around the N-FLAP' probe. (b) Relative energy of N-FLAP'(S₁)@Low MW PS in the ONIOM (TD-CAM-B3LYP/6-31+G(d):MM) calculations.

that the ONIOM (TD-CAM-B3LYP/6-31+G(d):MM) calculation provided a reasonable interpretation of the observed single-molecule FL behavior of N-FLAP in the low MW PS. When the total energy of N-FLAP'(S₁)@Low MW PS was plotted by changing the COT bending angle θ of N-FLAP' every 5 degree, local energy minima were obtained at which N-FLAP' takes an almost planar geometry ($\theta = 5^\circ$) and a bent geometry ($\theta = 30^\circ$) (Figure 9b). Due to the confined space in the host polymer, completely planar N-FLAP'(S₁) geometry (most relaxed in the gas phase) did not give an energy minimum of N-FLAP'(S₁)@Low MW PS. This result suggested that the relaxed N-FLAP'(S₁) geometry depends on the specific shape of the temporarily appeared void space, and therefore the spectral form of the green FL band have a structural variety (Figure 6 and Figure S24). The predicted energy barrier between bent and planar conformations of N-FLAP'(S₁) in the polymer is also consistent with the clear FL switch between the blue and green forms, rather than a gradual shift of the FL peak.

It should be noted that the calculated volume (green void) in Figure 9a includes the so-called excess free volume ($V_{\text{free:exs}}$)¹ in addition to the volume swept out during the planarization (280 Å³; green part in Figure 8e). Since the excess free volume is spatially continuous, we cut it off by setting the radius of 10 Å from the center of N-FLAP' (see the calculation method in the SI). We also note that the hard-core van der Waals volume of N-FLAP' has been calculated as 455 Å³ and it was almost constant (454–456 Å³) regardless of the COT bending angle ($\theta = 0$ –50°). The hard-core volume is not included in the green void.

CONCLUSIONS

A nitrogen-embedded flapping molecule has been developed as a superior environment-sensitive dual fluorescent probe for single-molecule fluorescence spectroscopy. Nitrogen substitution on the flapping wings enabled efficient visible excitation, leading to high brightness (22 times) of the probe. A suppression of the photo-oxidation process also results in long-term observation in the single molecule study. The probe in the low molecular weight polystyrene ($T_g = 18$ °C) provided dynamic single-molecule fluorescence spectrum at 23 °C that frequently jumps to the long-wavelength form, originating from

the temporarily permitted excited-state planarization dynamics of the flapping probe in sufficiently large polymer free volume. In this way, the probe is capable of visualizing local free volume changes on the order of 280 \AA^3 on subsecond time scales for extended periods of time. Statistical analysis of the duration time in the short- and long-wavelength spectra demonstrated that it takes $10.4 \pm 0.5 \text{ s}$ on average for the large free volume to generate, while it lasts for $1.2 \pm 0.1 \text{ s}$ on average. MD simulations and the following QM/MM calculations, in which the probe molecule was treated as the QM model while polystyrene chains were treated as the MM model, supported the dynamic spectral behaviors and the rough estimation of the free volume. The use of single-molecule imaging techniques can, in principle, also provide 3-dimensional localization of the probe and enable position-dependent studies of the free volume dynamics. The parallelization of wide-field and spectral imaging would be a next challenge, as it has been only partially realized.⁴²

■ ASSOCIATED CONTENT

SI Supporting Information

The Supporting Information is available free of charge at <https://pubs.acs.org/doi/10.1021/jacs.1c06428>.

Experimental and theoretical details (PDF)

Accession Codes

CCDC 1987186 contains the supplementary crystallographic data for this paper. These data can be obtained free of charge via www.ccdc.cam.ac.uk/data_request/cif, or by emailing data_request@ccdc.cam.ac.uk, or by contacting The Cambridge Crystallographic Data Centre, 12 Union Road, Cambridge CB2 1EZ, UK; fax: + 44 1223 336033.

■ AUTHOR INFORMATION

Corresponding Authors

Shohei Saito – Graduate School of Science, Kyoto University, Sakyo-ku, Kyoto 606-8502, Japan; orcid.org/0000-0003-1863-9956; Email: s_saito@kuchem.kyoto-u.ac.jp

Martin Vacha – Department of Materials Science and Engineering, School of Materials and Chemical Engineering, Tokyo Institute of Technology, Meguro-ku, Tokyo 152-8552, Japan; orcid.org/0000-0002-5729-9774; Email: vacha.m.aa@m.titech.ac.jp

Authors

Yuma Goto – Department of Materials Science and Engineering, School of Materials and Chemical Engineering, Tokyo Institute of Technology, Meguro-ku, Tokyo 152-8552, Japan

Shun Omagari – Department of Materials Science and Engineering, School of Materials and Chemical Engineering, Tokyo Institute of Technology, Meguro-ku, Tokyo 152-8552, Japan

Ryuma Sato – Cellular and Molecular Biotechnology Research Institute, National Institute of Advanced Industrial Science and Technology (AIST), Koto-ku, Tokyo 135-0064, Japan; orcid.org/0000-0003-2523-8966

Takuya Yamakado – Graduate School of Science, Kyoto University, Sakyo-ku, Kyoto 606-8502, Japan; orcid.org/0000-0002-0730-2904

Ryo Achiwa – Graduate School of Science, Kyoto University, Sakyo-ku, Kyoto 606-8502, Japan

Nilanjan Dey – Graduate School of Science, Kyoto University, Sakyo-ku, Kyoto 606-8502, Japan; Present

Address: Department of Chemistry, Birla Institute of Technology and Sciences-Pilani, Hyderabad, Telangana 500078, India.; orcid.org/0000-0002-3988-1509

Kensuke Suga – Graduate School of Science, Kyoto University, Sakyo-ku, Kyoto 606-8502, Japan

Complete contact information is available at:

<https://pubs.acs.org/10.1021/jacs.1c06428>

Notes

The authors declare no competing financial interest.

■ ACKNOWLEDGMENTS

JST PRESTO (FRONTIER) and JST FOREST Grant Numbers JPMJPR16P6 (S.S.) and JPMJFR201L (S.S.), JSPS KAKENHI Grant Numbers JP21H01917 (S.S.), JP19H02684 (M.V.), and JSPS Fellowships Grant Numbers JP19J22034 (T.Y.) and JP18F18335 (N.D.), and Toray Science Foundation (S.S.). We thank Prof. Hideki Yorimitsu (Kyoto University) for his help with the high-resolution mass spectrometry measurement. R.S. was supported by a special postdoctoral researcher program at RIKEN. The computations were performed at the Research Center for Computational Science (RCCS) in the Institute of Molecular Science (Okazaki, Japan) and the HOKUSAI (RIKEN).

■ REFERENCES

- (1) White, R. P.; Lipson, J. E. G. Polymer Free Volume and Its Connection to the Glass Transition. *Macromolecules* **2016**, *49*, 3987–4007.
- (2) Low, Z.-X.; Budd, P. M.; McKeown, N. B.; Patterson, D. A. Gas Permeation Properties, Physical Aging, and Its Mitigation in High Free Volume Glassy Polymers. *Chem. Rev.* **2018**, *118*, 5871–5911.
- (3) Dlubek, G.; Pointek, J.; Bondarenko, V.; Pompe, G.; Taesler, C.; Petters, K.; Krause-Rehberg, R. Positron Annihilation Lifetime Spectroscopy (PALS) for Interdiffusion Studies in Disperse Blends of Compatible Polymers: A Quantitative Analysis. *Macromolecules* **2002**, *35*, 6313–6323.
- (4) Yampolskii, Y. P.; Kaliuzhnyi, N. E.; Durgarjan, S. G. Thermodynamics of Sorption in Glassy Poly(vinyltrimethylsilane). *Macromolecules* **1986**, *19*, 846–850.
- (5) Golemme, G.; Nagy, J. B.; Fonseca, A.; Algieri, C.; Yampolskii, Y. ¹²⁹Xe-NMR study of free volume in amorphous perfluorinated polymers: comparison with other methods. *Polymer* **2003**, *44*, 5039–5045.
- (6) Victor, J. G.; Torkelson, J. M. On Measuring the Distribution of Local Free Volume in Glassy Polymers by Photochromic and Fluorescence Techniques. *Macromolecules* **1987**, *20*, 2241–2250.
- (7) Itagaki, H.; Horie, K.; Mita, I. Luminescent probe studies of the microstructure and mobility of solid polymers. *Prog. Polym. Sci.* **1990**, *15*, 361–424.
- (8) Strehmel, B.; Strehmel, V.; Younes, M. Fluorescence Probes for Investigation of Epoxy Systems and Monitoring of Crosslinking Processes. *J. Polym. Sci., Part B: Polym. Phys.* **1999**, *37*, 1367–1386.
- (9) Jansen, J. C.; Macchione, M.; Tocci, E.; De Lorenzo, L.; Yampolskii, Y. P.; Sanfirova, O.; Shantarovich, V. P.; Heuchel, M.; Hofmann, D.; Drioli, E. Comparative Study of Different Probing Techniques for the Analysis of the Free Volume Distribution in Amorphous Glassy Perfluoropolymers. *Macromolecules* **2009**, *42*, 7589–7604.
- (10) Vallée, R. A. L.; Cotlet, M.; Van Der Auweraer, M.; Hofkens, J.; Müllen, K.; De Schryver, F. C. Single-Molecule Conformations Probe Free Volume in Polymers. *J. Am. Chem. Soc.* **2004**, *126*, 2296–2297.

- (11) Wöll, D.; Braeken, E.; Deres, A.; De Schryver, F. C.; Uji-I, H.; Hofkens, J. Polymers and Single Molecule Fluorescence Spectroscopy, What Can We Learn? *Chem. Soc. Rev.* **2009**, *38*, 313–328.
- (12) Deres, A.; Floudas, G. A.; Müllen, K.; Van der Auweraer, M.; De Schryver, F. C.; Enderlein, J.; Uji-i, H.; Hofkens, J. The Origin of Heterogeneity of Polymer Dynamics near the Glass Temperature as Probed by Defocused Imaging. *Macromolecules* **2011**, *44*, 9703–9709.
- (13) Paeng, K.; Kaufman, L. J. Single Molecule Experiments Reveal the Dynamic Heterogeneity and Exchange Time Scales of Polystyrene near the Glass Transition. *Macromolecules* **2016**, *49*, 2876–2885.
- (14) Oba, T.; Vacha, M. Relaxation in Thin Polymer Films Mapped across the Film Thickness by Astigmatic Single-Molecule Imaging. *ACS Macro Lett.* **2012**, *1*, 784–788.
- (15) Habuchi, S.; Sato, N.; Yamamoto, T.; Tezuka, Y.; Vacha, M. Multimode Diffusion of Ring Polymer Molecules Revealed by a Single-Molecule Study. *Angew. Chem., Int. Ed.* **2010**, *49*, 1418–1421.
- (16) Ito, S.; Itoh, K.; Pramanik, S.; Takatsugu, K.; Takei, S.; Miyasaka, H. Evaluation of Diffusion Coefficient in a Dextrin-Based Photo-Curable Material by Single Molecule Tracking. *Appl. Phys. Express* **2009**, *2*, 075004.
- (17) Wöll, D.; Uji-i, H.; Schnitzler, T.; Hotta, J.; Dedecker, P.; Herrmann, A.; De Schryver, F. C.; Müllen, K.; Hofkens, J. Radical Polymerization Tracked by Single Molecule Spectroscopy. *Angew. Chem., Int. Ed.* **2008**, *47*, 783–787.
- (18) Ueda, K.; Aizawa, M.; Shishido, A.; Vacha, M. Real-Time Molecular-Level Visualization of Mass Flow during Patterned Photopolymerization of Liquid-Crystalline Monomers. *NPG Asia Mater.* **2021**, *13*, 25.
- (19) Kotani, R.; Sotome, H.; Okajima, H.; Yokoyama, S.; Nakaike, Y.; Kashiwagi, A.; Mori, C.; Nakada, Y.; Yamaguchi, S.; Osuka, A.; Sakamoto, A.; Miyasaka, H.; Saito, S. Flapping Viscosity Probe That Shows Polarity-Independent Ratiometric Fluorescence. *J. Mater. Chem. C* **2017**, *5*, 5248–5256.
- (20) Behera, S. K.; Park, S. Y.; Gierschner, J. Dual Emission: Classes, Mechanisms and Conditions. *Angew. Chem., Int. Ed.* **2021**, 9789.
- (21) Kimura, R.; Kitakado, H.; Osuka, A.; Saito, S. Flapping Peryleneimide as a Fluorescent Viscosity Probe: Comparison with BODIPY and DCVJ Molecular Rotors. *Bull. Chem. Soc. Jpn.* **2020**, *93*, 1102–1106.
- (22) Yang, S. K.; Shi, X.; Park, S.; Ha, T.; Zimmerman, S. C. A Dendritic Single-Molecule Fluorescent Probe That Is Monovalent, Photostable and Minimally Blinking. *Nat. Chem.* **2013**, *5*, 692–697.
- (23) Laha, J. K.; Tummalapalli, K. S. S.; Gupta, A. Palladium-Catalyzed Domino Double *N*-Arylations (Inter- and Intramolecular) of 1,2-Diamino(hetero)arenes with *o,o'*-Dihalo(hetero)arenes for the Synthesis of Phenazines and Pyridoquinoxalines. *Eur. J. Org. Chem.* **2013**, *2013*, 8330–8335.
- (24) Kimura, R.; Kuramochi, H.; Liu, P.; Yamakado, T.; Osuka, A.; Tahara, T.; Saito, S. Flapping Peryleneimide as a Fluorogenic Dye with High Photostability and Strong Visible-Light Absorption. *Angew. Chem., Int. Ed.* **2020**, *59*, 16430–16435.
- (25) Yamakado, T.; Takahashi, S.; Watanabe, K.; Matsumoto, Y.; Osuka, A.; Saito, S. Conformational Planarization versus Singlet Fission: Distinct Excited-State Dynamics of Cyclooctatetraene-Fused Acene Dimers. *Angew. Chem., Int. Ed.* **2018**, *57*, 5438–5443.
- (26) Wu, S. Chain Structure and Entanglement. *J. Polym. Sci., Part B: Polym. Phys.* **1989**, *27*, 723–741.
- (27) Livadaru, L.; Netz, R. R.; Kreuzer, H. J. Stretching Response of Discrete Semiflexible Polymers. *Macromolecules* **2003**, *36*, 3732–3744.
- (28) Quirk, R. Anionic Polymerization. In *Handbook of Polymer Synthesis, Characterization, and Processing*; Saldívar-Guerra, E., Vivaldo-Lima, E., Eds.; John Wiley & Sons: 2013; pp 127–162.
- (29) Kotani, R.; Liu, L.; Kumar, P.; Kuramochi, H.; Tahara, T.; Liu, P.; Osuka, A.; Karadakov, P. B.; Saito, S. Controlling the S₁ Energy Profile by Tuning Excited-State Aromaticity. *J. Am. Chem. Soc.* **2020**, *142*, 14985–14992.
- (30) Yamakado, T.; Otsubo, K.; Osuka, A.; Saito, S. Compression of a Flapping Mechanophore Accompanied by Thermal Void Collapse in a Crystalline Phase. *J. Am. Chem. Soc.* **2018**, *140*, 6245–6248.
- (31) Liu, J.; Deng, Q.; Jean, Y. C. Free-Volume Distributions of Polystyrene Probed by Positron Annihilation: Comparison with Free-Volume Theories. *Macromolecules* **1993**, *26*, 7149–7155.
- (32) Roland, C. M.; Casalini, R. Temperature Dependence of Local Segmental Motion in Polystyrene and Its Variation with Molecular Weight. *J. Chem. Phys.* **2003**, *119*, 1838–1842.
- (33) Chen, J.; Kistemaker, J. C. M.; Robertus, J.; Feringa, B. L. Molecular Stirrers in Action. *J. Am. Chem. Soc.* **2014**, *136*, 14924–14932.
- (34) Schroyers, W.; Vallée, R.; Patra, D.; Hofkens, J.; Habuchi, S.; Vosch, T.; Cotlet, M.; Müllen, K.; Enderlein, J.; De Schryver, F. C. Fluorescence Lifetimes and Emission Patterns Probe the 3D Orientation of the Emitting Chromophore in a Multichromophoric System. *J. Am. Chem. Soc.* **2004**, *126*, 14310–14311.
- (35) Böhmer, M.; Enderlein, J. Orientation Imaging of Single Molecules by Wide-field Epifluorescence Microscopy. *J. Opt. Soc. Am. B* **2003**, *20*, 554–559.
- (36) Patra, D.; Gregor, I.; Enderlein, J. Image Analysis of Defocused Single-Molecule Images for Three-Dimensional Molecule Orientation Studies. *J. Phys. Chem. A* **2004**, *108*, 6836–6841.
- (37) Zondervan, R.; Kulzer, F.; Berkhout, G. C. G.; Orrit, M. Local Viscosity of Supercooled Glycerol near T_g Probed by Rotational Diffusion of Ensembles and Single Dye Molecules. *Proc. Natl. Acad. Sci. U. S. A.* **2007**, *104*, 12628–12633.
- (38) Flier, B. M. I.; Baier, M. C.; Huber, J.; Müllen, K.; Mecking, S.; Zumbusch, A.; Wöll, D. Heterogeneous Diffusion in Thin Polymer Films as Observed by High-Temperature Single-Molecule Fluorescence Microscopy. *J. Am. Chem. Soc.* **2012**, *134*, 480–488.
- (39) Lin, H.; Truhlar, D. G. QM/MM: what have we learned, where are we, and where do we go from here? *Theor. Chem. Acc.* **2007**, *117*, 185–199.
- (40) Senn, H.; Thiel, W. QM/MM methods for biomolecular systems. *Angew. Chem., Int. Ed.* **2009**, *48*, 1198–1229.
- (41) Durrant, J. D.; Votapka, L.; Sørensen, J.; Amaro, R. E. POVME 2.0: An Enhanced Tool for Determining Pocket Shape and Volume Characteristics. *J. Chem. Theory Comput.* **2014**, *10*, 5047–5056.
- (42) Zhang, Z.; Kenny, S. J.; Hauser, M.; Li, W.; Xu, K. Ultrahigh-Throughput Single-Molecule Spectroscopy and Spectrally Resolved Super-resolution Microscopy. *Nat. Methods* **2015**, *12*, 935–938.